Wiley Online Library
Early View publication on www.wileyonlinelibrary.com
(issue and page numbers not yet assigned;
citable using Digital Object Identifier – DOI)

J. Biophotonics 1–11 (2016) / **DOI** 10.1002/jbio.201500209

Journal of BIOPHOTONICS

FULL ARTICLE

Pre-conditioning with near infrared photobiomodulation reduces inflammatory cytokines and markers of oxidative stress in cochlear hair cells

Adam Bartos[1], *Yohann Grondin*[1], *Magda E. Bortoni*[1], *Elisa Ghelfi*[1], *Rosalinda Sepulveda*[1], *James Carroll*[2], *and Rick A. Rogers*[*, 1]

[1] Harvard University – Harvard T.H. Chan School of Public Health, Molecular and Integrative Physiological Sciences – Department of Environmental Health, Building 1, 665 Huntington Ave Boston, MA, 02115, USA
2 THOR Photomedicine Ltd, Chesham, HP5 1LF, United Kingdom

Received 7 August 2015, revised 11 December 2015, accepted 12 December 2015
Published online 21 January 2016

Key words: Hearing loss, near-infrared, inflammation, oxidative stress, auditory cells, LLLT, Low Level Laser Therapy, near infrared photobiomodulation

Hearing loss is a serious occupational health problem worldwide. Noise, aminoglycoside antibiotics and chemotherapeutic drugs induce hearing loss through changes in metabolic functions resulting in sensory cell death in the cochlea. Metabolic sequelae from noise exposure increase production of nitric oxide (NO) and Reactive Oxygen Species (ROS) contributing to higher levels of oxidative stress beyond the physiologic threshold levels of intracellular repair. Photobiomodulation (PBM) therapy is a light treatment involving endogenous chromophores commonly used to reduce inflammation and promote tissue repair. Near infrared light (NIR) from Light Emitting Diodes (LED) at 810 nm wavelength were used as a biochemical modulator of cytokine response in cultured HEI-OC1 auditory cells placed under oxidative stress. Results reported here show that NIR PBM at 810 nm, 30 mW/cm^2, 100 seconds, 1.0 J, 3 J/cm^2 altered mitochondrial metabolism and oxidative stress response for up to 24 hours post treatment. We report a decrease of inflammatory cytokines and stress levels resulting from NIR applied to HEI-OC1 auditory cells before treatment with gentamicin or lipopolysaccharide. These results show that cells pretreated with NIR exhibit reduction of proinflammatory markers that correlate with inhibition of mitochondrial superoxide, ROS and NO in response to continuous oxidative stress challenges. Non-invasive biomolecular down regulation of proinflammatory intracellular metabolic pathways and suppression of oxidative stress via NIR may have the potential to develop novel therapeutic approaches to address noise exposure and ototoxic compounds associated with hearing loss.

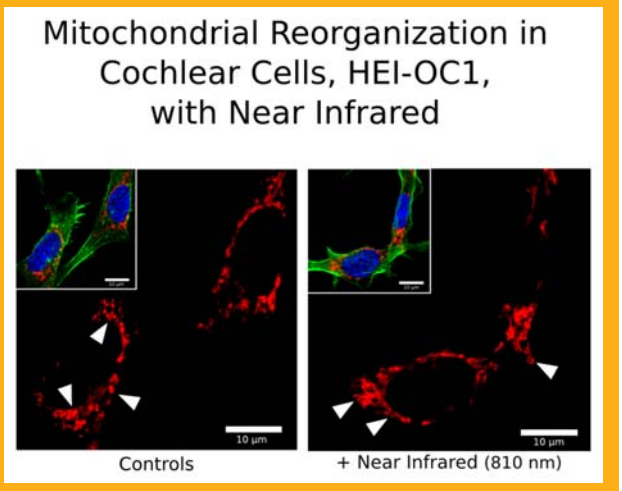

* Corresponding author: e-mail: rogers@bioimage.harvard.edu

1. Introduction

Noise-induced hearing loss (NIHL) is a prevalent occupational health injury [1] where genetic and environmental factors play a role [2, 3]. NIHL is often manifested as a loss of hair cells consequent to the activation of oxidative stress and inflammatory pathways resulting from noise exposure. When cochlear hair cells are exposed to noise or dangerous sounds, these primary sensory cells undergo excessive levels of oxidative stress predisposing them to cellular injury and death.

Hearing loss also can be caused by ototoxic aminoglycoside antibiotics, such as gentamicin and platinum-based chemotherapeutic drugs [4–7] that cause alterations in cellular tolerance to oxidative stress conditions. Therefore, it has been shown that noise exposure coincides with increased gentamicin uptake in cochlear hair cells further promoting hearing loss [8].

Noise and ototoxic injury of the cochlea resulting from the accumulation of Reactive Oxygen Species (ROS) molecules during oxidative stress leads to cochlear inflammation and auditory hair cell loss [9, 10]. Although ROS play a key role in cochlear metabolism and signal transduction under normal physiologic conditions, their overproduction induce an oxidative stress response that damages auditory cells and causes hearing loss in a number of animal models [11].

The increased accumulation of ROS and decreased level of natural antioxidant capacity of the cells leads to oxidative stress. The key ROS molecules are the hydroxyl radical ($OH^{\bullet}$), hydrogen peroxide (H_2O_2) and superoxide anion ($O_2^{\bullet -}$). Excess ROS molecules cause peroxidation of cell components such as lipids, proteins, and DNA [12] resulting in cochlear hair cell death and hearing loss [13]. Of particular interest is superoxide which is generated by oxidative stress that can react with nitric oxide (NO) (which is a signaling molecule at low concentrations but is produced at high concentrations by activated inflammatory cells) and form highly reactive peroxynitrite (ONOO–) Reactive Nitrogen Species (RNS). ROS and RNS molecules act together to damage the cells and cause nitrosative stress [14], an alternate pathway that also results in cellular damage.

Another caveat to the problem of excess ROS produced by oxidative stress are the observations shown to trigger signaling pathways that increase inflammation through elevation of proinflammatory cytokine levels such as IL-1β, IL-6 and TNF-α [15–17]. Other reports have shown elevated proinflammatory cytokines in outer hair cells appear to generate an immune response [18, 19] leading to cochlear inflammation.

Efforts to mitigate oxidative stress using antioxidants have shown promising results against NIHL in animal models, as these compounds can cross the blood-labyrinth barrier in limited amounts to control oxidative stress [20, 21] and prevent cochlear hair cell loss [22–29]. However in humans, otoprotection by antioxidants has not been fully realized and exploration of alternative non-invasive solutions are necessary. One approach we have been investigating utilizes application of near infrared light (NIR).

Light from the ultraviolet to infrared wavelengths within the electromagnetic spectrum have been used as effective therapeutic modalities in medicine. The ultraviolet range has been used to treat skin disorders such as psoriasis and vitiligo [30]. Blue light phototherapy is standard care for neonatal jaundice [31], whereas red light is used to activate some cancer therapeutic drugs in the field of Photodynamic Therapy (PDT) [32, 33]. Ultraviolet and most of the visible light spectrum will not penetrate much past the skin except in the far red/near infrared range. Many laboratory experiments and clinical trials in the red and infrared range have shown beneficial effects because they not only penetrate many mm up to a few centimeters but also are able to excite intracellular molecules.

The use of light in the visible red to near infrared range of the spectrum with light emitting diodes and low energy lasers is soon to receive the official title of Photobiomodulation therapy (PBM) Therapy. Previously, it was frequently referred to as low level laser/light therapy (LLLT), but the National Library of Medicine (best known globally for http://www.ncbi.nlm.nih.gov/pubmed/) will be giving it an official description and Medical Subject Heading (MeSH) at the end of November 2015 [34, 35]. PBM therapy has been used to promote tissue repair, reduce inflammation and reduce pain by triggering intracellular and extra cellular signaling pathways, and stimulating cellular metabolism, motility and proliferation [36, 37]. PBM has been shown to promote proliferation of fibroblasts, macrophages, mast cells, endothelial cells, keratinocytes, and many immune cells as well as peripheral and CNS neurons [38]. PBM has not been shown to have any of the carcinogenic and mutagenic properties [39] induced by ultraviolet therapies, this is because the red and near infrared photons have less energy than UV photons so the structure of DNA structure is not disturbed.

Exposure to low power non-invasive near infrared light (NIR) at wavelengths ranging from 700 nm to 1400 nm have been efficacious to mitigate oxidative stress and overcome inflammation in a variety of organ systems. Several early studies suggest that PBM with NIR can be useful in wound and retinal healing [40, 41], promotion of muscle regeneration [42], protection against neurotoxic compounds [43, 44], induction of neuroprotective effect *in vivo* [45],

pain relief through analgesia [46, 47], suppression of chronic joint pain [48], and reduction of symptoms of rheumatoid arthritis [49]. Pre-conditioning with NIR light has also been shown to be a useful tool to reduce damage caused by heart attack [50].

The mechanisms by which NIR works remain an active area of basic research. A common theory supported experiments suggests the role of the Cytochrome *c* Oxidase as a photoacceptor and key enzyme of respiratory chain mitochondria in PBM [38]. Cytochrome *c* Oxidase plays a key role in mitochondrial respiration and electron transport and contains a binuclear copper center and heme binuclear center [51] making this enzyme a uniquely available and responsive target for NIR. Cytochrome *c* Oxidase dysfunction is associated with increased NO production. NO has been established as an important signaling molecule, although excess NO could interact with the metal center of proteins and enzymes, such as the binuclear center CuB/a3 of Cytochrome *c* Oxidase [52]. The competitive binding between NO and O_2 leads to oxidative stress and lowers ATP production [53]. Previous studies suggested that one of the possible mechanisms by which PBM has an effect on cellular respiration is the photo dissociation of NO. Replacing NO with O_2 by PBM may result in increased ATP production and recovery in cellular respiration [54], although the mechanism of how PBM affects Cytochrome *c* Oxidase is remain unclear.

PBM directly mediates oxidative stress with the reduction of ROS molecules on cortical neurons [55], activates transcription factors such as NF-κB which have a complex role in the expression of proinflammatory genes [56]. PBM also decreases proinflammatory cytokine release in acute inflammatory phase response after muscle contusion [57]. It has been shown that PBM reduces the expression of iNOS (inducible Nitric Oxide Synthase) in the organ of Corti in rats [58].

We hypothesize that NIR protects against oxidative stress and inflammation in cochlear hair cells. In this study, we investigated the effect of pre-conditioning of cells in vitro with NIR irradiation modulated oxidative stress, mitochondrial function and inflammation in HEI-OC1 cells derived from the organ of Corti from the mouse cochlea. Since this cell type is exquisitely sensitive to redox damage, we applied experimental conditions to induce oxidative stress using a bacterial toxin or an ototoxic drug. Cells were challenged with gentamicin, a widely used ototoxic aminoglycoside antibiotic that promotes the formation of ROS [59]; and lipopolysaccharide (LPS), a bacterial-derived endotoxin that stimulates the transcription and release of proinflammatory cytokines. The effect of NIR radiation on auditory cells and its otoprotective effect thereby ameliorating ROS levels as well as proinflammatory cytokines have been investigated in this report.

2. Materials and methods

2.1 Cell culture

Cochlear hair cells HEI-OC1 (House Ear Institute, Los Angeles, CA, USA) were cultured in either permissive or non-permissive conditions [60]. These immortalized cells originate from the organ of Corti of the "immortomouse" genetically engineered mouse strain and contain a temperature-sensitive mutant of SV40 large-T antigen allowing the cells to grow at permissive temperature (33 °C) and differentiate at non-permissive temperature (39 °C). In permissive conditions, cells were seeded on uncoated plastic tissue culture flasks and cultured at 33 °C in high-glucose Dulbecco's Eagle's medium (DMEM) containing 10% fetal bovine serum (FBS; Gibco BRL) and 50 U/mL mouse IFN-γ without antibiotics. In non-permissive conditions, cells were cultured at 39 °C, without IFN-γ, in high-glucose DMEM with 10% fetal bovine serum. Before every experiment, cells were placed in non-permissive conditions and incubated for 24 h. All experiments were performed at 80% confluence.

2.2 Near infrared light (NIR) exposure

To investigate the effect of NIR on cochlear cells, cultured HEI-OC1 cells were exposed to 810 nm near-infrared light using a custom "BioTHOR" plate illuminator (THOR Photomedicine Ltd, UK). The irradiation parameters are provided in Table 1. The power density was verified at the bottom of the culture well by a PM100D optical power meter (ThorLabs, Newton, NJ).

Cells were treated with NIR and returned to incubation at 39 °C. Exposure occurred 15 min before challenge with either gentamicin or LPS. All experiments were conducted in the recovery phase following NIR exposure.

Table 1 The near infrared irradiation parameters

Source	LED	
Power Φ (per well)	9.5	mW
Beam area (per well)	0.32	cm^2
Irradiance E	30	mW/cm^2
Fluence H	3	J/cm^2
Energy Q (per well)	0.95	J
Time	100	s

2.3 Gentamicin and LPS challenge

HEI-OC1 auditory cells in non-permissive conditions were stressed with either 200 μM gentamicin antibiotic (Cat# E737-20ML Amresco Solon, OH) or 10 ng/mL Lipopolysaccharide (LPS Cat# L5418-2ML Sigma-Aldrich St. Louis, MO). Oxidative stress challenge was induced by gentamicin or LPS 1 at μM for 1, 3, 6, or 24 h to cells following NIR exposure under non-permissive conditions in multiwell glass bottom plates (Cat# #353219 Corning, Germany), then assayed.

2.4 Detection of oxidative stress and mitochondrial markers for Flow Cytometry

Oxidative stress characterization was performed *in vitro* using fluorescent cell-permeable dyes. Intracellular ROS levels were measured by cell permeable dye CellROX and DCF-DA (Life Technologies Grand Island, NY); intracellular NO levels by specific marker DAF-FM (Life Technologies Grand Island, NY); mitochondrial superoxide by MitoSOX (Life Technologies Grand Island, NY) and the superoxide levels by dihydroethidium (HE), (Life Technologies Grand Island, NY). All fluorescent dyes were applied in 1 μM concentration at non-permissive conditions in multiwell glass-bottom plates for 1 hour. Cells were then washed with 100 μl of media then detached with 100 μl of Accutase (BD Biosciences, San Jose, CA) for 10 min. Data evaluated by flow cytometry (BD Accuri C6 BD Biosciences, San Jose, CA)

MitoTracker Deep Red FM was purchased from Thermo Scientific (Cat. No. M22426) After 30 min of stress, 100 μL of media containing 100 nM of MitoTracker Deep Red FM were added to each well to achieve a final concentration of 50 nM. After 30 min, media removed and cells washed once with fresh media. Cells were detached with either 30 μL of trypsin for 3 min followed by 70 μL of 10% FBS in culture media to inactivate trypsin or with 100 μL of Accutase for 10 min. Cell detachment was aided by pipetting and samples were run in the 96 well plate using the BD Accuri C6 equipment with BD CSampler (BD Biosciences, San Jose, CA) and analyzed with FlowJo software (FlowJo LLC, Ashland, OR). For each assay, total fluorescent intensity of live gated cells was measured.

2.5 Detection of inflammatory markers

Evaluation of proinflammatory cytokines IL-6 and IL-1β expression was determined by multiplex magnetic bead–based immunoassay (Bio-Plex MAGPIX Multiplex Reader, Bio-Rad Waltham, MA). Radio Immunoprecipitation Assay (RIPA) buffer (Cat# 5871 Cell Signaling Danvers, MA) was used to prepare cell lysate, which were made at 1.2 mg/mL protein concentration. Samples were processed according to the manufacturer's protocol. Concentration of cytokine expression (pg/mL) from the samples were calculated with standard curves generated from Bio-Plex Pro Mouse Cytokine Standard 23-plex (Group 1 protein standard, Lot# 5036298). Cytokine detection range was defined by the lower and upper limit of quantification, typically from few pg/mL to 44 ng/mL.

2.6 Microscopic imaging and stereology analysis

To conduct this assay, 24-well black glass bottom plates were seeded with 50,000 cells per well in 1 mL of media and incubated overnight at 39 °C. The next day cells were treated with NIR and further incubated for 10 min. After incubation, media was substituted with 500 μL of prewarmed media containing 250 nM of MitoTracker Deep Red FM. Cells were further incubated for 1 hour at 39 °C, then washed 3× with PBS (3 min per wash) and fixed with 4% paraformaldehyde for 10 min. Cells were washed 2× with PBS and 500 μL of a 1 : 100 solution of Alexa Fluor 488 Phalloidin (Thermo Scientific, Cat. No. A12379) were added per well and incubated for 1 h at room temperature to detect actin cytoskeleton which we used as a general cell boundary marker for florescent microscopy. Cells were washed 2× with PBS and a drop of ProLong Gold Antifade Mountant with DAPI (Thermo Scientific, Cat. No. P36935) were added to each well. Cells were analyzed using a Zeiss LSM 700 confocal microscope. Images of stained cells were recorded using a plan/Apochromat 63×/1.40 objective lens. DAPI was detected with a 405 nm laser, phalloidin with a 488 nm laser and MitoTracker Deep Red FM with a 639 nm laser. All images were acquired using Zen Black software (Zeiss).

To evaluate changes in mitochondrial redistribution among the treatments, stereologic analysis was performed on 48 fields of view from NIR-exposed cells and 61 fields of view from control cells, with each field containing 1–4 cells. Two quantitative analyses were performed: (1) the mitochondrial area-to-cell ratio, which was calculated as the ratio of mitochondrial point counts divided by the total number of point counts per cell and (2) the mitochondrial surface to volume ratio, which was performed using a Merz pattern and calculated as the ratio of total number of intersections to total number of point count of mitochondrial profiles [61].

2.7 Statistical analysis

For reactive oxidative stress and mitochondrial markers, data consisted of duplicate experiments with $n = 4$. Homogeneity of variance was tested for each data using Levene's test for equality of variance. According to the result of that test, statistical analysis was performed using one-way ANOVA or Welch ANOVA followed by independent two-tailed *t*-tests or Welch's *t*-tests with Šídák Correction, respectively. Cytokine data consisted of four to 6 repeats and were analyzed with one-tailed *t*-tests. Values of $P < 0.05$ were considered as statistically significant. The analysis was performed with R version 3.1.2 [62] and CAR statistical analysis package [63]. Results are expressed as means ± standard error of means (SEM). Stereologic analysis was performed using image analysis software FIJI [64]. Means of mitochondrial area-to-cell ratios were compared with a two-tailed Student's *t*-test. The surface-to-volume ratio between NIR and controls was compared by bootstrapping with two-tailed using R version 3.1.2 [62].

3. Results

3.1 NIR reduces oxidative stress

To evaluate the potential of NIR to mitigate oxidative stress in the cochlea, we measured ROS levels using flow cytometry in HEI-OC1 cells challenged with gentamicin or LPS. Exposure to either drug significantly increased cellular ROS measured by CellROX, which remained high from within 1 h to

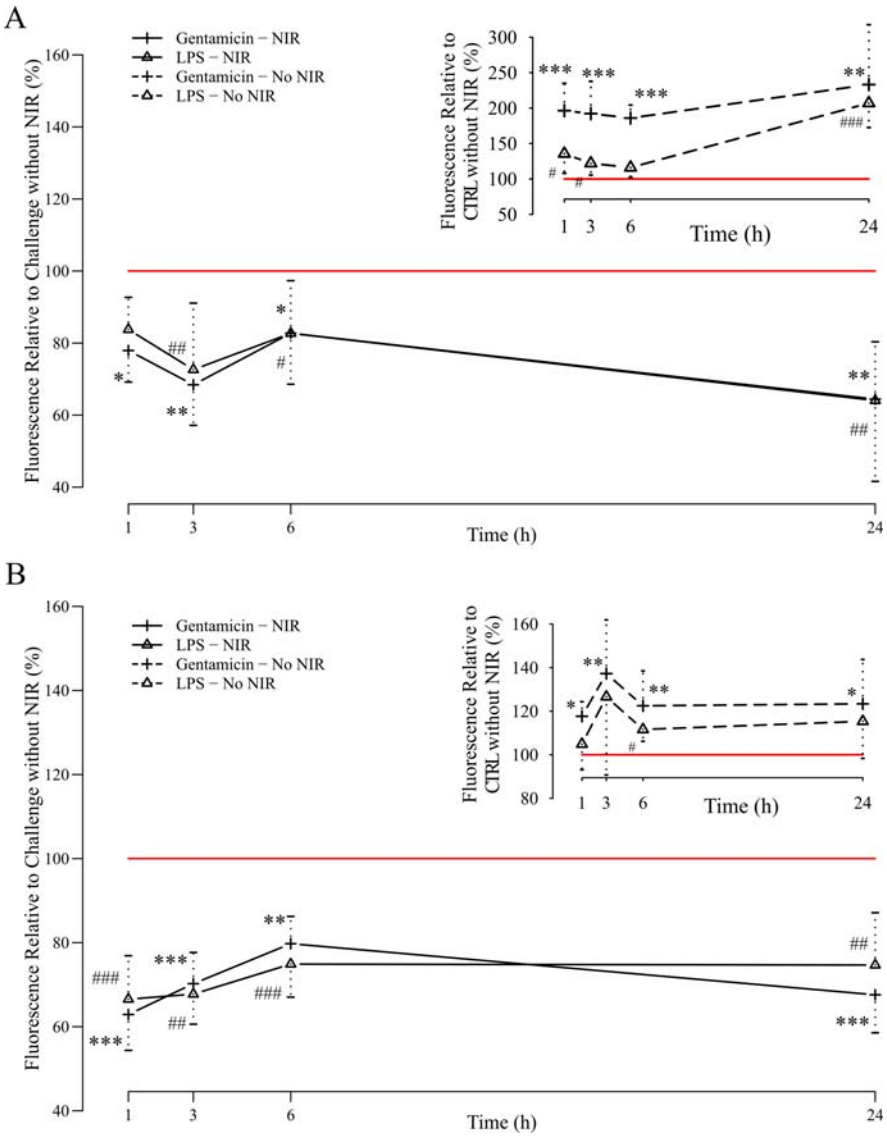

Figure 1 NIR reduces ROS levels in cells challenged with gentamicin or LPS. ROS levels determined by flow cytometry and quantified by the fluorescent intensity of CellROX (**A**) and DCF-DA (**B**) in HEI-OC1 cells exposed to NIR (full line) and treated with gentamicin (cross) or LPS (triangle) compared to non-exposed cells (red full line). Data were normalized to fluorescence intensity measured in non-NIR exposed HEI-OC1 cells treated with gentamicin or LPS, respectively. (Inset) Effect of stress in cells not exposed to NIR. Fluorescence intensity after gentamicin or LPS treatment normalized with non-treated cells (CTRL, red full line) measured by CellROX (inset A) and DCF-DA (inset B). All data show the average of 2 experimental repeats ($n = 4$ per repeat) with SEM. Significant differences to controls shown with levels 0.05 (*, #), 0.01 (**, ##) and 0.001 (***, ###) with Šídák correction for gentamicin and LPS, respectively.

24 h of challenge (Figure 1A). However, this increase was reduced by pre-exposing cells for 100 s to NIR, 15 min before challenge. In both gentamicin- and LPS-challenged cells, mean fluorescent intensity of ROS markers significantly decreased up to about 35% (Figure 1A), compared to challenged cells without NIR treatment. In non-challenged cells exposed to NIR, ROS showed an 18% to 48% decrease in relative fluorescence. These results were confirmed using DCF-DA, another ROS marker, with a decrease of ROS ranging from 20% to 38% in relative fluorescence after NIR exposure (Figure 1B).

To further examine the effect of NIR on ROS response, we measured in both the mitochondrial and the cytoplasmic compartments, changes in superoxide, a well-known ROS, that functions as a substrate to other ROS. Similar to the ROS results shown above, mitochondrial superoxide quantified by MitoSOX fluorescent dye was elevated after gentamicin or LPS challenge in cells not exposed to NIR (Figure 2A inset) while pre-exposing the cells to NIR prevented that increase completely (Figure 2A).

Cytoplasmic superoxide measured by dihydroethidium was also elevated after gentamicin or LPS challenge (Figure 2B). However, conversely to mitochondrial superoxide, prevention of superoxide production by NIR was marginal and only observable at 6 h and 24 h under persist gentamicin challenge (Figure 2B). NIR significantly decreased superoxide production over 24 h by 10% to 40% relative fluorescence in cells under gentamicin chal-

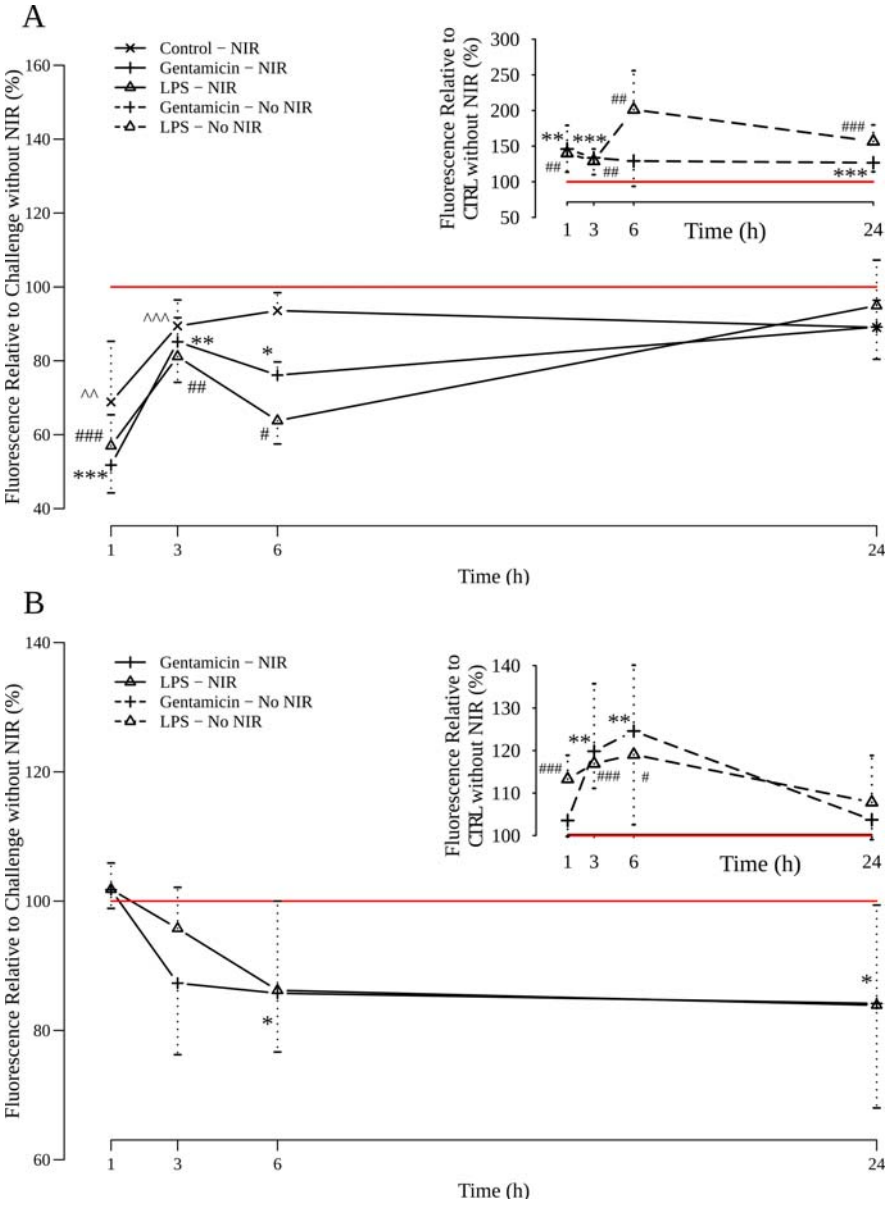

Figure 2 Effect on NIR on superoxide. Mitochondrial superoxide levels (**A**) and cellular superoxide level (**B**) was measured by flow cytometry and presented as the fluorescent intensity. Mitochondrial superoxide levels was measured by MitoSOX in HEI-OC1 cells exposed to NIR (full line) in non-treated cells (circle) and in cells treated with gentamicin (cross) or LPS (triangle) compared to non-exposed cells (red full line). Data were normalized to fluorescence intensity measured in non-NIR exposed cells with no treatment or treated with gentamicin or LPS, respectively. (Inset) Effect of stress in cells not exposed to NIR. Fluorescence intensity after gentamicin or LPS treatment normalized with non-treated cells (CTRL, red full line) measured by MitoSOX.

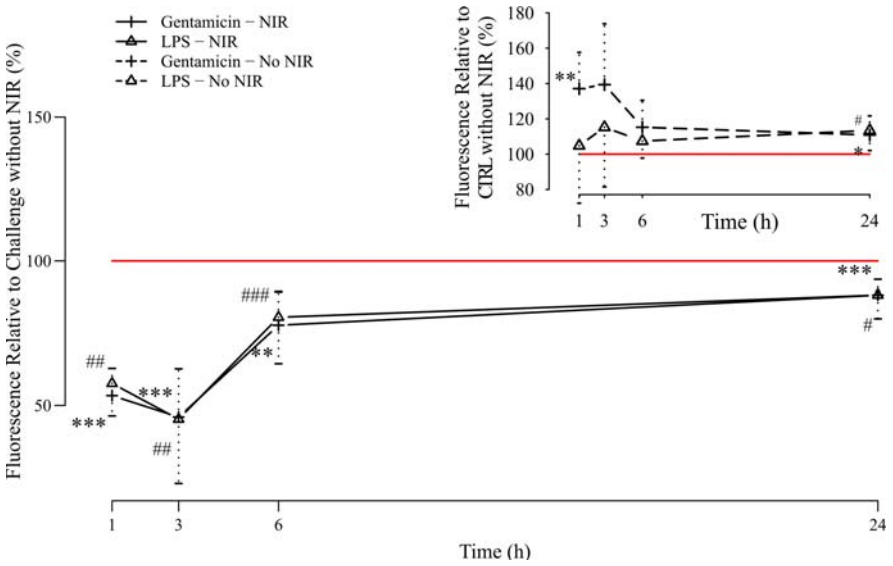

Figure 3 NIR reduces NO levels in cells gentamicin or LPS stress. Cellular superoxide levels determined by flow cytometry and the fluorescence intensity was quantified by DAF-FM in HEI-OC1 cells exposed to NIR (full line) and treated with gentamicin (cross) or LPS (triangle) compared to non-exposed cells (red full line). Data were normalized to fluorescence intensity measured in non-NIR exposed cells treated with gentamicin or LPS, respectively. (Inset) Effect of stress in cells not exposed to NIR. Fluorescence intensity after gentamicin or LPS treatment normalized with non-treated cells (CTRL, red full line) measured by DAF-FM. All data show the average of 2 experimental repeats (n = 4 per experiment) with SEM. Significant differences to controls shown with levels 0.05 (*, #), 0.01 (**, ##) and 0.001 (***, ###) with Šídák correction for gentamicin and LPS, respectively.

lenge, and by 20% to 40% relative fluorescence in cells under LPS challenge. The reduction in superoxide production (10–30%) was also observed in non-challenged cells exposed to NIR.

3.2 NIR exposure reduces NO level

To evaluate the role of NIR in modulating signaling response, NO levels were measured using DAF-FM.

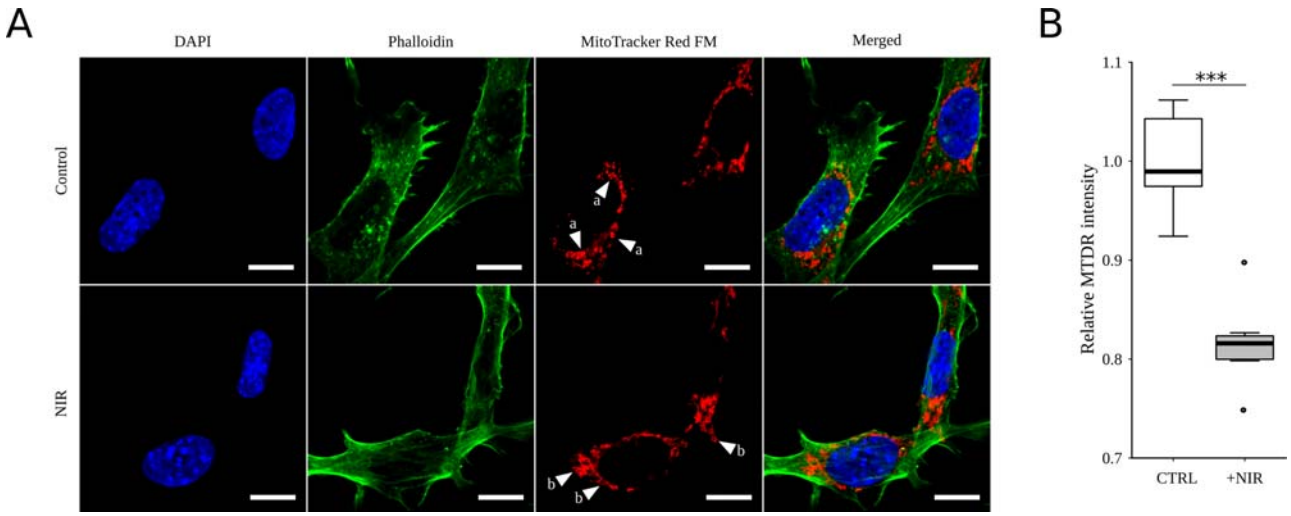

Figure 4 NIR effect on mitochondrial redistribution is represented by fluorescent confocal microscopy. (**A**) Mitochondrial redistribution in HEI-OC1 cells exposed to NIR was compared to controls (no NIR). Cells were stained with fluorescent dye MitoTracker Red FM, counterstained with DAPI and Phalloidin and imaged by confocal microscopy. Resulting images were merged to form a color composite. In control cells (top row), mitochondria showed rounded and disconnected structures (a arrowheads). In cells exposed to NIR (bottom row), mitochondria showed elongated interconnected structures (b arrowheads). The images are representative of the results in each experimental condition. White scale bars represent 10 μm. (**B**) Active mitochondrial level was determined by BD Accuri C6 equipment with BD CSampler flow cytometer and quantified by the fluorescent intensity of MitoTracker Deep Red FM. Data was analyzed with FlowJo software (FlowJo LLC, Ashland, OR). For each assay, total fluorescent intensity of live gated cells were measured.

Table 2 Stereology analyses. The mitochondrial area-to-cell ratio was calculated as the ratio of mitochondrial point counts divided by the total number of point counts per cell. The mitochondrial surface to volume ratio, Sv, was performed using a Merz pattern and calculated as the ratio of total number of intersections, I, to total number of point count of mitochondrial profiles, P [61], such $Sv = A\Sigma I/\Sigma P$, with $A = 2p/l$ and p/l the cycloid length per point [61]. N.S (non-significant).

	Control	NIR	Significance
Mitochondrial area-to-cell ratio	0.11	0.13	N.S
Surface to volume ratio (Sv)	7.63 A	10.2 A	$p < 0.05$

Despite a limited effect of gentamicin or LPS on NO levels in cells not exposed to NIR (Figure 3), NIR significantly decreased NO over 24 h post exposure period (t-test with Šídák correction, $p < 0.5$). Cells pre-exposed to NIR had from 12% to 55% lower NO in comparison to cells not exposed to NIR for either gentamicin or LPS stress (Figure 3), with a low peak at 3 h post-exposure.

3.3 NIR exposure reduces active mitochondria

Interestingly, NIR reduced the intensity of the mitochondrial marker, MitoTracker Deep Red FM, which accumulates in active mitochondria proportional to the mitochondrial membrane potential. We observed structural reorganization of the mitochondria in NIR-exposed cells; Mitochondria in control cells showed more rounded disconnected features whereas mitochondria in NIR-exposed cells had smaller connected structures (Figure 4A). The mitochondrial surface to volume ratio significantly increased in cells exposed to NIR ($p < 0.05$, two-sided), consistent with the change in structure (rounded structure are expected to have smaller surface to volume ratio). The ratio of mitochondria to cell area showed no difference between NIR and control cells ($p > 0.05$, two-sided t-test) (Table 2). The significant reduction in the number of metabolically active mitochondria was observed 1 hour after NIR exposure (Figure 4B).

3.4 NIR exposure reduces proinflammatory cytokine expression

To further investigate the bio-modulating effect of NIR upon inflammation response in HEI-OC1 cells, the cytokines IL-1β and IL-6 in cell lysates were analyzed after 24 h of challenge from gentamicin or LPS exposure. In cells not exposed to NIR, levels of IL-1β and IL-6 significantly increased in both gentamicin and LPS challenges (Figure 5). Consistent with the proinflammatory effect of LPS, IL-1β and IL-6 levels were 2 to 3 times higher than in those cells treated with gentamicin. For both cytokines, NIR pre-exposure significantly reduced IL-1β and IL-6, compared to cells not exposed to NIR (Figure 5).

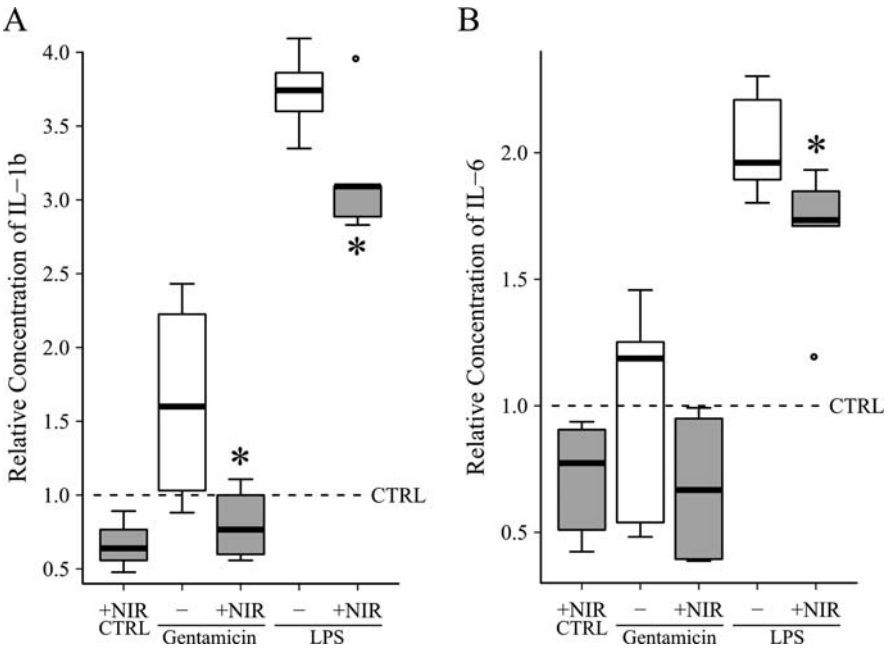

Figure 5 Proinflammatory cytokine reduction 24 h after NIR exposure. Reduction of proinflammatory cytokine Il-1β (**A**) and IL-6 (**B**) in lysates of cells pre-exposed to NIR (grey) in comparison to controls cells (white). Cells were either untreated (CTRL) or challenged 24 h with gentamicin or LPS. All data are normalized to cells non-challenged and non-exposed to NIR (CTRL, dashed line) with $*p < 0.05$. Data was acquired by MAGPIX multiplex system.

4. Discussion

Our results suggest that NIR affects mitochondrial superoxide and cellular ROS while leaving cytoplasmic superoxide unchanged in cells exposed to gentamicin and LPS. This indicates NIR functions to regulate superoxide to reduce the amount of ROS expressed in cells. Previous data have shown that ROS increase, following gentamicin treatment *in vitro*, inhibited glutathione peroxidase and glutathione reductase, two enzymes responsible for the restoration of glutathione levels and removal of H_2O_2 [65]. Determination of whether NIR prevents gentamicin from inhibiting these enzymes or, on the contrary, results in a limitation of ROS production rate will require further investigation.

Previous studies showed that PBM increase survival of cochlear hair cell numbers and mediates their recovery after acoustic or gentamicin-induced trauma in rats *in vivo* [66, 67]. However, recovery is only partial and mainly benefits cells in the middle turn of the cochlea [67], yet the mechanism driving oxidative stress and modulating inflammatory pathways remain unclear. Our investigation introduces a better understanding of the mechanistic feature of NIR applied to cochlear hair cells and show that NIR reduces ROS, and suppresses proinflammatory mediators. Furthermore, we report this effect persist for up to 24 hours post treatment.

In our studies thus far, we observe decreased NO levels accompanied reduced oxidative stress levels following a single dose of NIR irradiation. These findings suggest that NIR irradiation of auditory hair cells diminish excess NO production and alters redox activity because excess NO production leads to oxidative stress. Superoxide is a substrate to other ROS molecules. Superoxide radical reacts with NO and form peroxynitrite molecule which block cellular respiration and diminish ATP production [53].

NIR reduced the levels of proinflammatory cytokines IL-1β and IL-6 in HEI-OC1 auditory cells challenged with either gentamicin or LPS. Expression of these proinflammatory cytokines is the first step of the immune response and an indicator of cochlear inflammation. These results are consistent with observations in other studies in which cell types exposed to NIR wavelengths [68] and support the anti-inflammatory potential of NIR in hearing loss. It has been reported that long term inflammation correlates with hearing loss [69] and expression of inflammatory cytokines IL-1b and IL-6 in the inner ear increase shortly after noise exposure [70, 71]. Cochlear inflammation appears to correlate with the capability to recover from hearing loss injuries [72]. Importantly, blocking IL-6 signaling appears to suppress inner ear inflammation and reduces noise induced hearing loss [73] highlighting the contribution of inflammation to hearing loss.

The significance of altered cytokine profiles in auditory hair cells could influence the restricted blood flow in stria vacularis following noise exposure. The microvasculature component supporting the stria vascularis is responsible for maintenance of the endolymphatic potential necessary for hair cell contractility. Localized inflammation can alter blood flow in this sensitive capillary system resulting in decreased potassium levels leading to impairment of cochlear function. Dyfunctional cochlear environment produced by restricted blood flow would lead to increased oxidative stress that would produce a redox inbalance in mitochondrial superoxide expression and cellular ROS formation.

NIR treatment diminished ROS formation and oxidative stress accompanied with the decreased number of active mitochondria. The increased number of active mitochondria, as a consequence of oxidative stress, has been previously described [74]. Although perinuclear redistribution of mitochondria after PBM irradiation has been previously reported in osteoblastic cells [75], the mechanism of NIR irradiation-induced perinuclear redistribution of mitochondria needs further examination.

NIR has been shown to be a beneficial therapeutic tool and has been FDA-approved for treatment of adjunctive pain therapy [76], carpal tunnel syndrome [77] and alopecia [78] of specific conditions. The advantage of this non-invasive tool is of great interest in context with cochlear otoprotection since the cochlea is not easily accessible, physically or pharmacologically.

5. Conclusion

Our results show that NIR exposure mitigates oxidative stress response in HEI-OC1, a cochlea-derived cell line, challenged with gentamicin or LPS by modulating mitochondrial activity, mitochondrial superoxide, cellular ROS and NO levels. In addition, NIR exposure was correlated with a reduction in the production of proinflammatory cytokines IL-1β and IL-6. These results suggest that NIR applied to auditory cells in situ may represent an effective tool to control and limit cochlear oxidative stress and induction of localized cochlear inflammation within the organ of Corti. Thus making NIR a potential therapeutic candidate to address high levels of oxidative stress in cochlear auditory cells exposed to ototoxic drugs such as gentamicin or resulting from occupational noise exposure. The efficiency and safety of NIR makes it also suitable for consideration in other medical applications such as prevention of hearing loss.

Acknowledgements The authors would like to gratefully acknowledge funding from the Office of Naval Research,

awards; N000141310794 and N000141210170 awarded to Dr. Rick A. Rogers. We acknowledge the contributions made by K. Yankaskas for his critical review of the conceptual framework, the experimental design and data. The authors would also like to thank F. Kalinec for generously providing HEI-OC1 cells. J. Carroll has a declared financial conflict of interest. All other authors declare no financial conflict of interest.

Author biographies Please see Supporting Information online.

References

[1] D. I. Nelson, R. Y. Nelson, M. Concha-Barrientos, and M. Fingerhut, Am. J. Ind. Med. **48**, 446–458 (2005).
[2] M. Sliwinska-Kowalska and M. Pawelczyk, Mutat. Res. **752**, 61–65 (2013).
[3] Y. Grondin, M. E. Bortoni, R. Sepulveda, E. Ghelfi, A. Bartos, D. Cotanche, R. E. Clifford, and R. A. Rogers, PLoS One **10**, e0130827 (2015).
[4] D. Henderson, S. L. McFadden, C. C. Liu, N. Hight, and X. Y. Zheng, Ann. N. Y. Acad. Sci. **884**, 368–380 (1999).
[5] D. Henderson, E. C. Bielefeld, K. C. Harris, and B. H. Hu, Ear Hear **27**, 1–19 (2006).
[6] H. Li and P. S. Steyger, Noise Health **11**, 26–32 (2011).
[7] H. Li, Q. Wang, and P. S. Steyger, PLoS One **6**, e19130 (2011).
[8] D. Ding, B. L. Allman, and R. Salvi, Anat. Rec. **295**, 1851–1867 (2012).
[9] K. K. Ohlemiller, Brain Res. **1091**, 89–102 (2006).
[10] T. R. van de Water, C. T. Dinh, R. Vivero, G. Hoosien, A. A. Eshraghi, and T. J. Balkany, Acta Otolaryngol. **130**, 308–311 (2010).
[11] C. Fujimoto and T. Yamasoba, Oxid. Med. Cell. Longev. **2014**, 582849 (2014).
[12] D.-F. Dai, Y. A. Chiao, D. J. Marcinek, H. H. Szeto, and P. S. Rabinovitch, Longev. Heal. **3**, 6 (2014).
[13] B. H. Hu, D. Henderson, and T. M. Nicotera, Hear. Res. **166**, 62–71 (2002).
[14] A. Poirrier, J. Pincemail, P. Van Den Ackerveken, P. P. Lefebvre, and B. Malgrange, Curr Med Chem. 173591–173604 (2010).
[15] W. Huang and C. K. Glass, Arterioscler. Thromb. Vasc. Biol. **30**, 1542–1549 (2010).
[16] C. Gomez, L. Martinez, A. Mesa, J. C. Duque, L. A. Escobar, S. M. Pham, and R. I. Vazquez-Padron, Biosci. Rep. **35**, e00227 (2015).
[17] C.-Y. Tseng, J.-F. Chang, J.-S. Wang, Y.-J. Chang, M. K. Gordon, and M.-W. Chao, PLoS One **10**, e0131911 (2015).
[18] H. Satoh, G. S. Firestein, P. B. Billings, J. P. Harris, and E. M. Keithley, JARO – J. Assoc. Res. Otolaryngol. **4**, 139–147 (2003).
[19] H. So, H. Kim, J. H. Lee, C. Park, Y. Kim, E. Kim, J. K. Kim, K. J. Yun, K. M. Lee, H. Y. Lee, S. K. Moon, D. J. Lim, and R. Park, JARO – J. Assoc. Res. Otolaryngol. **8**, 338–355 (2007).
[20] B. Nikooyeh and T. R. Neyestani, Diabetes Metab Res Rev., doi: 10.1002/dmrr.2718 (2015).
[21] Y. Grondin, D. A. Cotanche, O. Manneberg, R. Molina, J. H. Treviño-villarreal, R. Sepulveda, R. Clifford, M. E. Bortoni, S. Forsberg, B. Labrecque, L. Altshul, J. D. Brain, R. L. Jackson, and R. A. Rogers, Hear. Res. **298**, 93–103 (2013).
[22] M. G. Pierson and A. R. Møller, Hear. Res. **4**, 79–87 (1981).
[23] S. H. Sha and J. Schacht, Hear. Res. **142**, 34–40 (2000).
[24] D. Yamashita, H.-Y. Jiang, C. G. Le Prell, J. Schacht, and J. M. Miller, Neuroscience **134**, 633–642 (2005).
[25] K. C. M. Campbell, R. P. Meech, J. J. Klemens, M. T. Gerberi, S. S. W. Dyrstad, D. L. Larsen, D. L. Mitchell, M. El-Azizi, S. J. Verhulst, and L .F. Hughes, Hear. Res. **226**, 92–103 (2007).
[26] J. K. M. Coleman, R. D. Kopke, J. Liu, X. Ge, E. A. Harper, G. E. Jones, T. L. Cater, and R. L. Jackson, Hear. Res. **226**, 104–113 (2007).
[27] L. P. Rybak, C. A. Whitworth, D. Mukherjea, and V. Ramkumar, Hear. Res. **226**, 157–167 (2007).
[28] K. Campbell, A. Claussen, R. Meech, S. Verhulst, D. Fox, and L. Hughes, Hear. Res. **282**, 138–144 (2011).
[29] J. Lu, W. Li, X. Du, D. L. Ewert, M. B. West, C. Stewart, R. A. Floyd, and R. D. Kopke, JARO – J. Assoc. Res. Otolaryngol. **15**, 353–372 (2014).
[30] A. Sokolova, A. Lee, and S. D. Smith, Am J Clin Dermatol. **16**, 501–531 (2015).
[31] H. P. Schwartz, B. E. Haberman, and R. M. Ruddy, Pediatr Emerg Care **27**(9), 884–889 (2011).
[32] N. P. Brodin, C. Guha, and W. A. Tomé, Technol Cancer Res Treat **14**(4), 355–368 (2015).
[33] Y. S. Khaled, K. Wright, A. Melcher, and D. Jayne, Lancet **385**(1), S56 (2015).
[34] T. Karu, J Photochem Photobiol B **49**, 1–17 (1999).
[35] M. R. Hamblin and T. N. Demidova, Proceedings of SPIE 6140. pp. 614001-1–614001-12 (2006).
[36] J. T. Eells, M. T. Wong-Riley, J. VerHoeve, M. Henry, E. V. Buchman, M. P. Kane, L. J. Gould, R. Das, M. Jett, B. D. Hodgson, D. Margolis, and H. T. Whelan, Mitochondrion **4**, 559–567 (2004).
[37] W. P. Hu, J. J. Wang, C. L. Yu, C. C. Lan, G. S. Chen, and H. S. Yu, J Invest Dermatol **127**, 2048–2057 (2007).
[38] H. Chung, T. Dai, S. K. Sharma, Y.-Y. Huang, J. D. Carroll, and M. R. Hamblin, Ann. Biomed. Eng. **40**, 516–533 (2012).
[39] L. Marrot and J. R. Meunier, J Am Acad Dermatol **58** (5 Suppl 2), S139–148 (2008)
[40] M. J. Conlan, J. W. Rapley, and C. M. Cobb, J Clin Periodontol **23**, 492–496 (1996).
[41] W. Posten, D. A. Wrone, J. S. Dover, K. A. Arndt, S. Silapunt, and M. Alam, Dermatol. Surg. **31**, 334–340 (2005).
[42] N. Weiss and U. Oron, Anat Embryol (Berl) **186**, 497–503 (1992).
[43] M. T. Wong-Riley, X. Bai, E. Buchmann, and H. T. Whelan, Neuroreport **12**, 3033–3037 (2001).

[44] M. T. Wong-Riley, H. L. Liang, J. T. Eells, B. Chance, M. M. Henry, E. Buchmann, M. Kane, and H. T. Whelan, J Biol Chem **280**, 4761–4771 (2005).
[45] J. C. Rojas, J. Lee, J. M. John, and F. Gonzalez-Lima, J Neurosci **28**, 13511–13521 (2008).
[46] E. Hahm, S. Kulhari, and P. R. Arany, Photonics Lasers Med. **1**, 241–254 (2012).
[47] C. Ferraresi, M. R. Hamblin, and N. A. Parizotto, Photonics Lasers Med. **1**, 267–286 (2012).
[48] J. M. Bjordal, C. Couppé, R. T. Chow, J. Tunér, and E. A. Ljunggren, Aust. J. Physiother. **49**, 107–116 (2003).
[49] A. Christie, G. Jamtvedt, K. T. Dahm, R. H. Moe, E. A. Haavardsholm, and K. B. Hagen, Phys. Ther. **87**, 1697–1715 (2007).
[50] T. Agrawal, G. K. Gupta, V. Rai, J. D. Carroll, and M. R. Hamblin, Dose Response **12**, 619–649 (2014).
[51] S. Farivar, T. Malekshahabi, and R. Shiari, J Lasers Med Sci. **5**, 58–62 (2014).
[52] G. C. Brown, Biochim Biophys Acta **1504**, 46–57 (2001).
[53] S. Srinivasan and N. G. Avadhani, Free Radic Biol Med. **15**, 1252–1263 (2012)
[54] J. T. Hashmi, Y. Y. Huang, B. Z. Osmani, S. K. Sharma, M. A. Naeser, and M. R. Hamblin, PM&R **2**, S292–305 (2010)
[55] Y.-Y. Huang, K. Nagata, C. E. Tedford, T. McCarthy, and M. R. Hamblin, J. Biophotonics **6**, 829–838 (2013).
[56] A. C.-H. Chen, P. R. Arany, Y.-Y. Huang, E. M. Tomkinson, S. K. Sharma, G. B. Kharkwal, T. Saleem, D. Mooney, F. E. Yull, T. S. Blackwell, and M. R. Hamblin, PLoS One **6**, e22453 (2011).
[57] P. De Almeida, S. S. Tomazoni, L. Frigo, P. D. T. C. de Carvalho, A. A. Vanin, L. A. Santos, and E. C. P. Leal-Junior, Lasers in Medical Science **29**, 653–658 (2013).
[58] A. Tamura, T. Matsunobu, K. Mizutari, K. Niwa, T. Kurioka, S. Kawauchi, S. Satoh, S. Hiroi, Y. Satoh, M. Nibuya, R. Tamura, and A. Shiotani, Neurosci. Lett. **595**, 81–86 (2015).
[59] J. Schacht, A. E. Talaska, and L. P. Rybak, Anat. Rec. (Hoboken) **295**, 1837–1850 (2012).
[60] G. M. Kalinec, P. Webster, D. J. Lim, and F. Kalinec, Audiol Neurootol **8**, 177–189 (2003).
[61] C. Suri, J. McClain, G. Thurston, D. M. McDonald, H. Zhou, E. H. Oldmixon, T. N. Sato, and G. D. Yancopoulos, Science (New York, N.Y.) **282**, 468–471 (1998).
[62] R Core Team (2014).
[63] J. Fox and S. Weisberg, An {R} Companion to Applied Regression, Second, Sage, Thousand Oaks {CA} (2011).
[64] J. Schindelin, I. Arganda-Carreras, and E. Frise, Nature methods **9**(7), 676–682 (2012).
[65] C. Acharya, H. Thakar, and S. Vajpeyee, Natl. J. Physiol. Pharm. Pharmacol. **3**, 14 (2013).
[66] C. K. Rhee, P. He, J. Y. Jung, J. C. Ahn, P. S. Chung, M. Y. Lee, and M. W. Suh, J Biomed Opt. **18**, 128003 (2013).
[67] C. K. Rhee, P. He, J. Y. Jung, J. C. Ahn, P. S. Chung, and M. W. Suh, Lasers Med Sci. **27**, 987–992 (2012).
[68] J.-Y. Wu, C.-H. Chen, C.-Z. Wang, M.-L. Ho, M.-L. Yeh, and Y.-H. Wang, PloS One **8**, e54067 (2013).
[69] S. D. Nash, K. J. Cruickshanks, W. Zhan, M. Y. Tsai, R. Klein, R. Chappell, F. J. Nieto, B. E. K. Klein, C. R. Schubert, D. S. Dalton, and T. S. Tweed, J. Gerontol. A. Biol. Sci. Med. Sci. **69**, 207–214 (2014).
[70] M. Fujioka, S. Kanzaki, H. J. Okano, M. Masuda, K. Ogawa, and H. Okano, J. Neurosci. Res. **83**, 575–583 (2006).
[71] K. Wakabayashi, M. Fujioka, S. Kanzaki, H. J. Okano, S. Shibata, D. Yamashita, M. Masuda, M. Mihara, Y. Ohsugi, K. Ogawa, and H. Okano, Neurosci. Res. **66**, 345–352 (2010).
[72] P. De Almeida, S. S. Tomazoni, L. Frigo, P. D. T. C. de Carvalho, A. A. Vanin, L. A. Santos, and E. C. P. Leal-Junior, Lasers in Medical Science **29**, 653–658 (2013).
[73] M. Fujioka, Y. Okamoto, S. Shinden, H. J. Okano, H. Okano, and K. Ogawa, PLoS One **9**, e90089 (2014).
[74] H. C. Lee, P. H. Yin, C. W. Chi, and Y. H. Wei, J Biomed Sci. **9**, 517–526 (2002).
[75] D. A. Pires Oliveira, R. F. de Oliveira, R. A. Zangaro, and C. P. Soares, Photomed Laser Surg. **4**, 401–404 (2008)
[76] Laser Health Technologies, LLC K100116, U.S. Food and Drug Administration (2010).
[77] M. N. Melkerson, K081166, U.S. Food and Drug Administration (2009).
[78] M. N. Melkerson, K091496, U.S. Food and Drug Administration (2010).